JOURNAL OF MATERIALS SCIENCE 17 (1982) 1789–1794

The properties of dynamically compacted Metglas® 2826

D. G. MORRIS
Institute CERAC, CH-1024, Ecublens, Switzerland

The dynamic compaction process has previously been shown to be suitable for the consolidation of rapidly-solidified and thermally-unstable materials with the retention of much of the metastability of the original powder. The mechanical and corrosion-resistance behaviour of compacted amorphous Metglas® 2826 has been determined and is compared here with that of the as-solidified material. Some loss of metastability always occurs during dynamic compaction which could be due to a complete loss of amorphism or due to a more minor structural change. Effective bonding between powder particles was obtained but a form of micro-porosity within the bond-zones appeared to affect material behaviour.

1. Introduction

The development of the dynamic compaction process and its application to rapidly-quenched materials has previously been reported [1–3]. The technique makes use of a high-pressure shock-wave, here generated by the impact of a fast moving projectile, which passes through the powder and thereby effects compaction. A careful balance is necessary between a sufficiently violent impact, for effective interparticle bonding and densification, and a limitation on the quantity of mechanical energy used, in order to avoid overheating and degradation of material structure and properties. Information on interparticle bond formation and the control of the heating–cooling cycle during compaction has also been reported [4], based on a study of the compaction of tool steel powder. Briefly, the surface deformation and heating occurring during compaction, leading sometimes to localized surface melting, is responsible for highly effective bonding between powder particles. Homogenization of the heat occurs very rapidly as heat is absorbed by the particle interiors. Subsequently, heat is lost much more slowly by the large compacted object to its surrounding container. The factors determining the temperature levels and heating and cooling rates have also been enumerated, and it has been shown that effective bonding can be achieved with only small temperature rises [4] and retention of the metastability of powders [2]. Little has been published to date about the properties of compacted metastable materials. The present work reports in detail on the properties of the compacted amorphous alloy Metglas® 2826 with particular attention to the extent of retention of as-solidified structure and properties.

2. Experimental details

Details of the dynamic compaction technique and the material and powder used have been given previously [2] and only a brief summary is given here. Dynamic compaction was carried out using a two-stage gas gun to launch plastic pistons which impacted onto powder held within a pressure container. Typical piston velocities and pressures were in the range 1000 to 2000 m sec^{-1} and 1 to 7 GPa, respectively, and the quantity of mechanical energy deposited within the powders led to temperature rises in the range 100° C to nearly 1000° C. The applied pressure did not appear to have an independent effect on the properties of compacted materials and these will be related uniquely to the extent of bonding and to the temperature rise occurring. The material used was the Metglas® 2826 alloy, purchased from Allied Chemical Corporation, in the form of strip about 50 μm thick and 2 mm wide. This strip was

0022–2461/82/061789–06$03.22/0

chopped to "powder" with pieces of length and width approximately 0.5 to 1 mm and thickness 50 μm.

Hardness measurements on the compacted materials were made on a Leitz Vickers hardness tester using a load of 100 g. Fracture toughness measurements were made on three-point bend test specimens, 20 mm x 5 mm x 2.5 mm, notched to half thickness at the centre. Tensile specimens of parallel gauge dimensions, length 6 mm, width 3 mm and thickness 1 mm, with shoulder radii of 3 mm, were spark-machined from compacted pieces and tested using a floor-mounted Instron machine with specially designed self-aligning grips. Fracture surfaces were examined by scanning electron microscopy using Cameca and Cambridge 250 machines.

The corrosion resistance was established by the measurement of current density at the specimen electrode as a function of the potential difference across an electrolytic cell. The electrolyte used was aerated 1M NaCl, with the same electrode surface area and separation for each comparative test performed. Testing began with no externally applied potential and the current was recorded as the potential slowly increased.

Unlubricated sliding wear tests were performed using a specially constructed test machine comprising a rotating steel drum of diameter 60 mm onto which a small flat piece of test material was pressed. The extent of wear was easily recorded by measuring the size of the wear surface. A special holder allowed the specimen to be removed from the drum for this measurement and to be replaced in exactly the same position. The technique had the disadvantage of measuring wear under conditions of continually decreasing applied stress as wear occurred, but was highly sensitive for the measurement of small amounts of wear and proved to be remarkably reproducible.

3. Results and discussion

3.1. Density

Measured densities of compacted glass were $(7.48 \pm 0.05) \times 10^3$ kg m^{-3}, corresponding to nearly 100% of the quoted density of the cast material (7.51×10^3 kg m^{-3}). The relatively low precision of measurement arises from the relatively small quantities of material used. Further estimates based on metallographic examinations confirmed that percentage densities above 99.8% theoretical were obtained.

3.2. Hardness

Hardness of as-compacted material are shown in Fig. 1, as a function of the temperature achieved during compaction. For the relatively small temperature rises, where microstructural examinations have shown that complete amorphism is retained, slight increases in hardness were observed. Increases in hardness while retaining complete amorphism have been recorded previously for other metallic

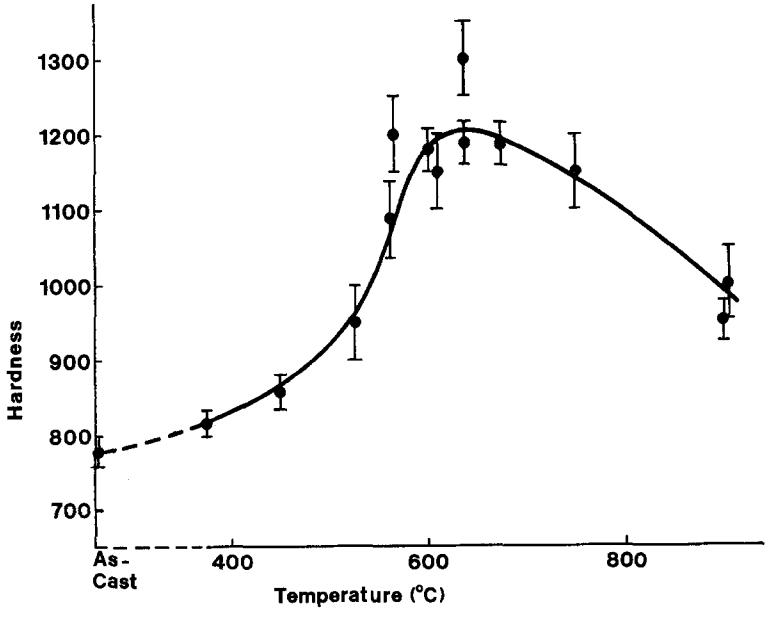

Figure 1 Hardness of as-compacted materials, plotted as a function of the temperature achieved during compaction.

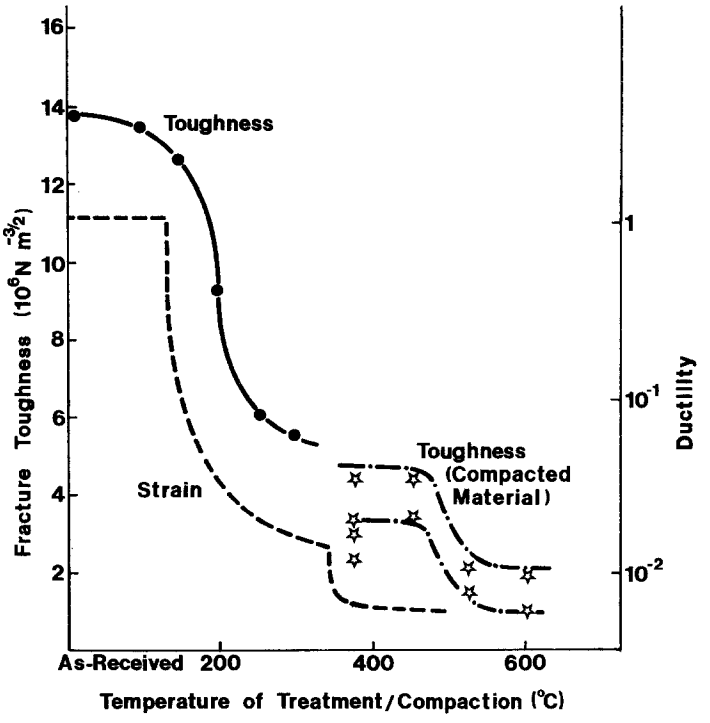

Figure 2 Toughness of compacted material, plotted as a function of compacting temperature and toughness and relative ductility of as-solidified and aged strip.

glasses, for example [5]. As crystallization takes place, a large increase in hardness occurs, while, for the very large temperature rises where over-ageing occurs, there is a fall in hardness of the as-compacted object.

3.3. Fracture behaviour

3.3.1. Toughness

The toughness of compacted material is compared with toughness and relative ductility measured on as-solidified or annealed strip [6–8] in Fig. 2. Both toughness and ductility of the strip fall after annealing at about 150 to 200° C (ageing for about 1 h) corresponding to the pre-crystallization embrittlement of this alloy, with a further fall near 350° C as crystallization occurs. The toughness of compacted material corresponds with that expected for strip at temperatures near crystallization. The increase in crystallization temperature to about 500° C has been shown to be a consequence of the short time-scale of the heat treatment during compaction [2, 3, 9]. The variability of toughness at any given compaction condition is caused by a variation in the extent of inter-particle bonding between specimens.

3.3.2. Tensile behaviour

During tensile testing the compacted material exhibited a near-elastic response up to the point where rapid fracture occurred. The tensile strengths recorded were of the order of one-half the values quoted for the as-solidified material [10]. This relatively low-strength brittle behaviour is believed to arise from a fracture-toughness limit and the presence of small cracks, or regions of imperfect bonding, between the plate-like powder particles.

3.3.3. Fracture surfaces

Fig. 3 shows most of the fracture surface of a toughness specimen. Fracture began from the

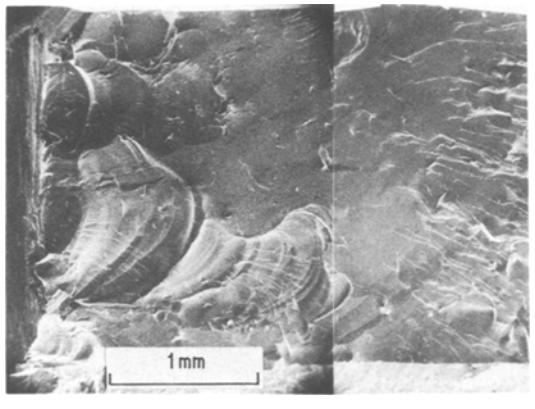

Figure 3 Fracture surface of compacted material. Notch is shown at left and the final fracture is near the right.

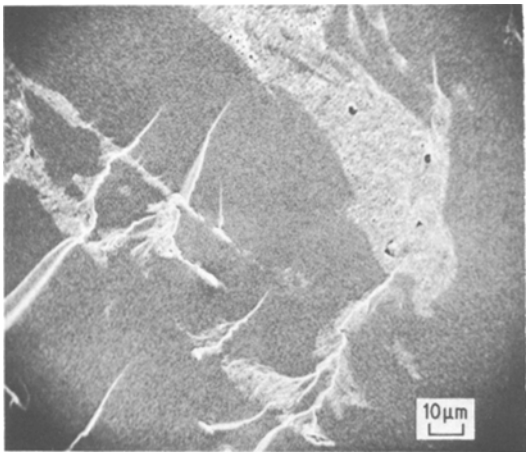

Figure 4 Fracture surface of compacted material showing the typical surface features observed.

notch (at left in Fig. 3) with the formation of several chip-like cracked areas. As the crack progressed (to right in Fig. 3) the surface became smoother with only occasional features visible. Subsequently, a build-up of fine-scale surface features occurred as final fracture approached. These characteristics of fracture are very similar to those observed on inorganic and polymeric glasses. Fig. 4 shows a higher magnification view of several of the features identified in Fig. 3. This fracture surface is generally flat and smooth, with several distinct classes of features visible:

(a) a relatively flat and speckled region with a fine distribution of pores about one micrometre or less in size;

(b) river-patterned tongues of material often starting at the porous regions and corresponding to tear regions between crack-fronts on slightly different levels; and

(c) occasional straight lines of imperfect interparticle bond-zones (more evident at left of Fig. 4).

Fig. 5 shows a transmission electron micrograph corresponding to the porous region of Fig. 4. No evidence of crystalline phases was found within these regions and it appears likely that the region corresponds to the melted bond-zone between powder particles and contains both microshrinkage porosity and entrapped surface oxides.

While, in general, the fracture surfaces indicated brittle behaviour and, indeed, on some occasions the Wallner line patterns observed on highly embrittled glasses were seen [11], for the specimen where particularly low compaction temperatures were maintained a more ductile fracture surface, interlaced with melt-pools, was observed (see Fig. 6).

Figure 5 Transmission electron micrograph of the porous melt-zone.

3.4. Corrosion resistance

Polarization curves both for as-solidified, aged and compacted samples of glass and for the mild steel are shown in Fig. 7. Higher current densities at a given applied potential correspond to faster chemical attack and the delay of the current density plateau to higher applied potential corresponds to increased resistance to attack. The as-solidified Metglas® 2826 alloy is seen to be highly resistant to attack and, while part of this resistance is lost by ageing to produce embrittlement (but no crystallization), this alone is insufficient to explain the poorer chemical resistance of the compacted material. This poorer resistance is explained by faster attack at the microstructural inhomogeneities within the material, namely the porous melt-zones and the intense slip bands produced during dyna-

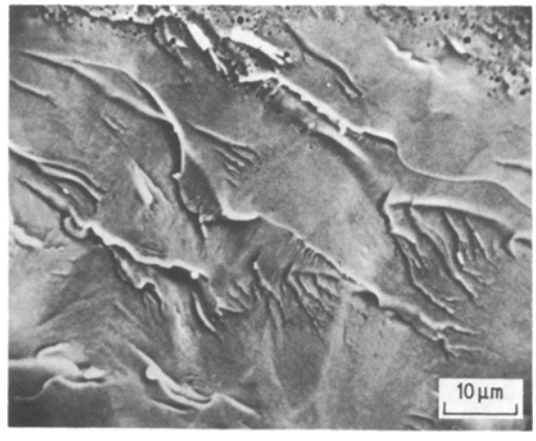

Figure 6 Fracture surface from a specimen of relatively ductile material.

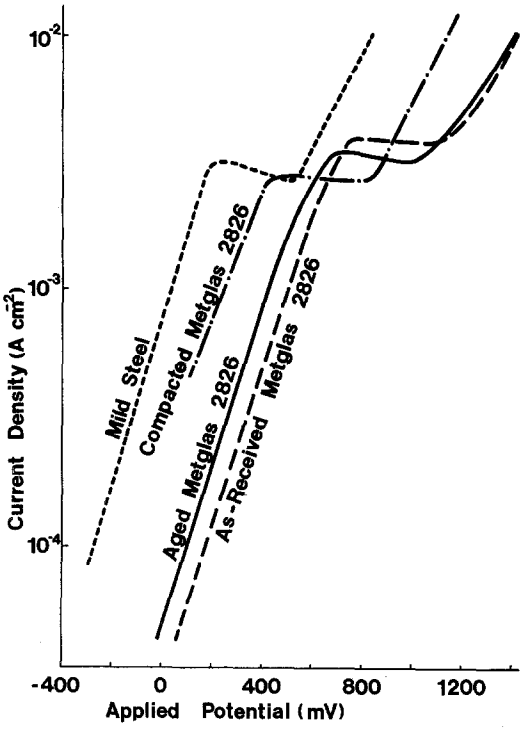

Figure 7 Polarization curves both for Metglas® 2826 in various states of preparation and for mild steel.

mic compaction, as confirmed by surface studies where there was evidence of preferential attack at such inhomogeneities.

3.5. Wear resistance

Wear tests on compacted materials are of particular interest in view of the possibility that amorphous materials may be useful in wear resisting situations. Furthermore, very little has been reported on the wear behaviour of such materials, either in the compacted or the as-solidified states.

In all cases the wear rate was initially high and decreased continuously at longer times. This feature is probably a characteristic of the measuring technique used, since the applied stress on the wearing surface continuously decreased as wear occured. The results, summarized in Figs 8 and 9, compare the behaviour of the compacted glass with those of an untreated and soft (hardness ~ 350 Hv) high-speed steel and a treated and hard (hardness ~ 900 Hv) high-speed steel. In each case two wear rates were recorded: the average wear rate over the first 5 km of sliding wear and the wear rate at the point where 5 km of sliding has occurred. The variations in both sets of data are similar and may be summarized as follows.

For the compacted glass the wear rate increased approximately linearly with the applied weight (Fig. 8). For all the materials tested, the wear increased with the sliding speed (Fig. 9); this may probably be taken as corresponding to greater wear at the higher surface temperatures generated. At low to medium sliding rates the compacted glass and hardened tool steel had similar wear rates while the soft tool steel wore at a considerably faster rate. At high sliding speeds the hardened tool steel retained reasonably good wear resistance while the amorphous alloy wore much faster, in fact at a rate comparable to that of the soft tool steel. This loss of wear resistance may be related to the lower thermal stability of the amorphous alloy, which will crystallize (and then over-age) at temperatures of about 400° C, while the hardened tool steel will remain stable up to temperatures of about 600° C.

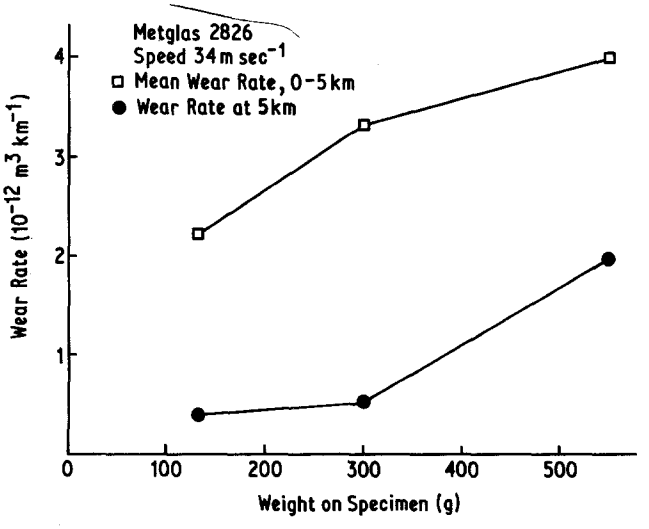

Figure 8 Unlubricated sliding wear rates of compacted glass, plotted as a function of applied load.

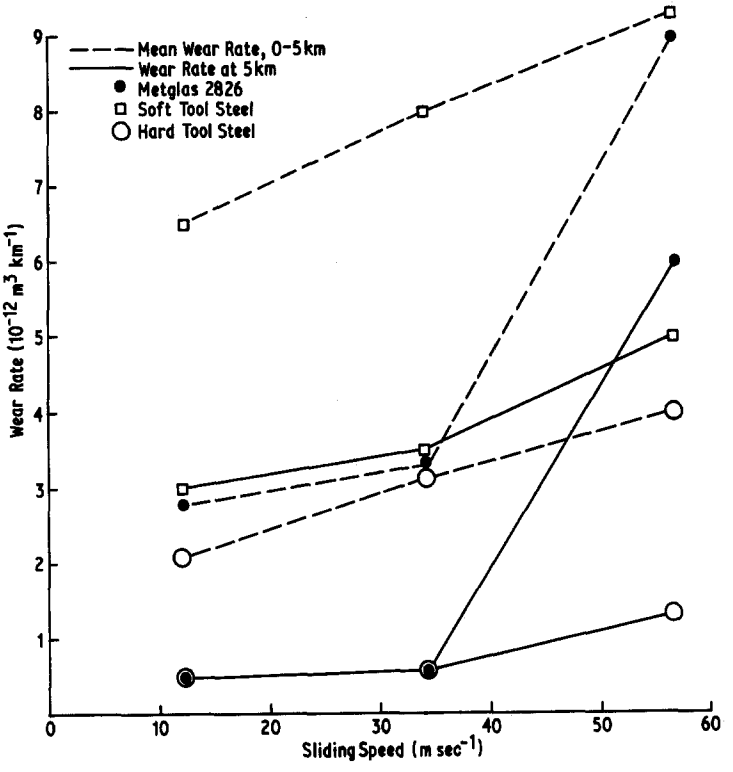

Figure 9 Unlubricated sliding wear rates of compacted glass and hardened and soft high-speed tool steel, plotted as a function of sliding speed.

4. Conclusions

This work has reported in detail the properties of dynamically compacted Metglas® 2826 and has shown that, to a large extent, effective consolidation can be achieved with a reasonably good retention of the desirable metastable properties observed in the as-solidified, ribbon state. The deformation behaviour is seen to be sensitive both to the pre-crystallisation embrittlement exhibited by this alloy and to the small regions of imperfect bonding present after compaction. Corrosion resistance of the compacted material was found to be similarly sensitive to such imperfections. The sliding wear behaviour of such a material has for the first time been reported and been shown to be extremely good under relatively mild wear conditions.

References

1. D. RAYBOULD, D. G. MORRIS and G. A. COOPER, *J. Mater. Sci.* **14** (1979) 2523.
2. D. G. MORRIS, *Metal Sci.* **14** (1980) 215.
3. D. RAYBOULD, *J. Mater. Sci.* **16** (1981) 589.
4. D. G. MORRIS, *Metal Sci.* **15** (1981) 116.
5. R. L. FREED, and J. B. VANDER SANDE, *Acta met.* **28** (1980) 103.
6. D. G. AST and D. KRENISTSKY, *Mater. Sci. Eng.* **23** (1976) 241.
7. L. A. DAVIS, in "Metallic Glasses" edited by J. J. Gilman and H. J. Leamy (American Society for Metals, Metals Park, Ohio, 1978) p. 190.
8. L. A. DAVIS, R. RAY, C. CHOU and R. C. O'-HANDLEY, *Scripta Met.* **10** (1976) 541.
9. D. G. MORRIS, *Acta Met.* **29** (1981) 1213.
10. D. J. KRENITSKY and D. G. AST, *J. Mater. Sci.* **14** (1979) 275.
11. A. KAURASHIMA, K. HASHIMOTO and T. MASUMOTO, *Scripta Met.* **14** (1980) 41.

Received 8 October
and accepted 10 November 1981